Intramolecular Energy Transfer in Bis-porphyrins Containing Diimine Chelates of Variable Geometry as Spacers

Graham Hungerford,[a] Mark Van der Auweraer,*[a] Jean-Claude Chambron,[b] Valérie Heitz,[b] Jean-Pierre Sauvage,*[b] Jean-Louis Pierre,*[c] and Dacil Zurita[c]

Abstract: Free-base porphyrin dimers bridged by either 6,6′-diphenyl-2,2′-bipyridine or 2,9-diphenyl-1,10-phenanthroline spacers were synthesized and characterized. Metallation of one of the porphyrins with Zn^{II} allowed us to study intramolecular energy-transfer processes between the Zn^{II}-porphyrin photoreceptor and the free-base porphyrin energy acceptor by time-correlated single-photon counting. The rate of energy transfer was shown to depend strongly on the nature of the bridge, being enhanced by a factor of nearly 6 when comparing the (*cis*) phenanthroline bridge with the *trans*-bipyridine bridge. A detailed analysis of the fluorescence decays suggests the presence of two slowly interconverting conformers for the 6,6′-diphenyl-2,2′-bipyridine spacer.

Keywords: energy transfer · fluorescence spectroscopy · porphrinoids · supramolecular chemistry · zinc

Introduction

In photosynthetic organisms, photoinduced electron transfer that induces conversion of light energy into chemical energy begins when photonic excitation has reached the so-called reaction center (RC). This process can be realized when the special pair (SP) of porphyrins belonging to the RC is directly excited, but it is more efficient when light excitation is trapped and transferred through a pool of well-organized bacteriochlorophyll (Bchl) chromophores included in the light-harvesting (LH) antenna protein. For example, in the bacteria *Rhodopseudomonas acidophila*, the light harvesting system (LH_2) is formed from two rings of noncovalently linked BChla, one consisting of nine pigments that absorb at 800 nm and the second one composed of eighteen chromophores that absorb at 850 nm.[1, 2] This highly organized structure of BChls enhances the spectral width of the energy trapped and the efficiency of energy transfer, since LH_2 funnels the energy towards the RC.

Energy-transfer processes between natural tetrapyrrolic chromophores has inspired many research groups. The models synthesized are composed of at least two porphyrins; often a zinc porphyrin is used as the energy donor and a free-base porphyrin as the energy acceptor. The porphyrins are linked covalently either by flexible hydrocarbon chains[3–5] or more rigid aliphatic or aromatic spacers.[6–11] Assembling porphyrins in a more biomimetic way was achieved by the use of either coordination bonds[12–16] or hydrogen bonds.[17, 18] In particular, multiporphyrin complex structures have been described as light-harvesting antenna models since 1993. All have in common four zinc porphyrins forming an external ring linked to a central free-base porphyrin. In Lindsey's system,[19] an acetylenic bridge to the central free-base porphyrin covalently links these zinc porphyrins. Sanders and McCallien[20] developed another synthetic route for their pentameric edifice. The free base 5,10,15,20-tetrakis-(4-pyridyl)porphyrin was used as a template to assemble four zinc dioxoporphyrins bearing acetylenic groups. The resulting complex was subsequently submitted to the Glaser–Hay coupling reaction to produce the cyclic covalently bound tetramer. Rempel and co-workers[21] also formed a pentamer by the use of the coordination properties of the same free-base porphyrin towards two covalently linked zinc(II) bis-porphyrins. Another way of forming the pentameric structure was to use the preformed macrocyclic structure of four zinc porphyrins as a receptor for the same free-base 5,10,15,20-tetrakis-(4-pyridyl)porphyrin. The aggregate made by Slone and Hupp[22] has a molecular

[a] Prof. M. Van der Auweraer, Dr. G. Hungerford
Laboratory for Molecular Dynamics and Spectroscopy, K. U. Leuven
Celestijnenlaan 200F, B-3001 Heverlee (Belgium)
Fax: (+32) 16-327990
E-mail: mark.vanderauweraer@chem.kuleuven.ac.be.

[b] Prof. J.-P. Sauvage, Dr. J.-C. Chambron, Dr. V. Heitz
Laboratoire de Chimie Organo-Minérale, UMR 7513 du CNRS
Université Louis Pasteur, Institut Le Bel, 4, rue Blaise Pascal
F-67070 Strasbourg Cedex (France)

[c] Prof. J.-L. Pierre, Dr. Dacil Zurita
Laboratoire d'Etudes Dynamiques et Structurales de la Sélectivité
URA D0332 du CNRS, Université Joseph Fourier, BP 53X
F-38041 Grenoble Cedex (France)

  0947-6539/99/0507-2089 $ 17.50+.50/0

square in which Zn^{II}-complexed 5,15-bis-(4-pyridyl)porphyrins placed at the edges are assembled with $[Re(CO)_3Cl]$ subunits, which form the corners. This molecular box coordinates the meso tetrapyridyl free-base porphyrin with a high association constant ($4 \times 10^7\,M^{-1}$). Sanders and co-workers[23] used a similar organic receptor, made from four Zn^{II} porphyrins covalently bridged by acetylenic spacers. This receptor complexes the same 5,10,15,20-tetrakis-(4-pyridyl)-porphyrin with a binding constant even greater ($2 \times 10^{10}\,M^{-1}$). The common feature of these pentameric arrays is the ability to function as an efficient energy collector and to show efficient, directed intramolecular energy transfer: light energy is absorbed by the external zinc–porphyrin macrocycle and transferred to the central free-base porphyrin.

Our approach was to study energy-transfer processes in dimers of porphyrins as a function of the distance and orientation of the two chromophores.[24] These were covalently linked by either 2,9-diphenyl-1,10-phenanthroline (phen) or 6,6′-diphenyl-2,2′-bipyridine (bipy) bridges. These two bridges have similar electronic properties, but the bipy permits free rotation about the 2,2′ carbon–carbon bond and has a preferred *trans* conformation, whereas phen is a planar and rigid spacer, which holds the two porphyrins in a *cis* conformation. The zinc/free-base porphyrin dimers allowed us to study the energy-transfer mechanism through dipole–dipole interactions according to Förster's theory and the dependence of distance and orientation on the rate of energy transfer.

Results and Discussion

Synthesis of the compounds of this study: The compounds of interest in this study are the bis-porphyrins Znphen2H (M_1 = Zn, M_2 = 2H) and Znbipy2H (M_1 = Zn, M_2 = 2H), see Figure 1. In Figure 1 the symmetrical bis-porphyrins 2Hphen2H, ZnphenZn, 2Hbipy2H, and ZnbipyZn are also represented. The porphyrin dimers 2Hphen2H and 2Hbipy2H were obtained in one-pot reactions by condensation of the dialdehyde spacers **1** and **2** (Figure 2), respectively, with the appropriate stoichiometry of 3,3′-diethyl-4,4′-dimethyl-2,2′-dipyrrylmethane (**4**) and 3,5-di-*tert*-butylbenzaldehyde (**3**) in

Abstract in French: *Des dimères de porphyrines bases libres liées par un espaceur de type 6,6′-diphényl-2,2′-bipyridine, ou de type 2,9-diphényl-1,10-phénanthroline ont été synthétisés et caractérisés. La complexation de l'une des porprhyrines des dimères par le Zn^{II} a permis d'étudier les processus de transfert d'énergie entre la porphyrine de zinc, capteur de photons et la porphyrine base libre, accepteur d'énergie, par la technique de comptage individuel de photons en fonction du temps. On montre que la vitesse de transfert d'énergie dépend fortement de la nature chimique de l'espaceur, étant augmentée d'un facteur de 6 quand on compare les résultats obtenus avec l'espaceur phénanthroline (cis) à ceux obtenus avec l'espaceur bipyridine (trans). Une analyse des déclins de fluorescence suggère que ce dernier donne lieu à deux conformères qui s'échangent lentement.*

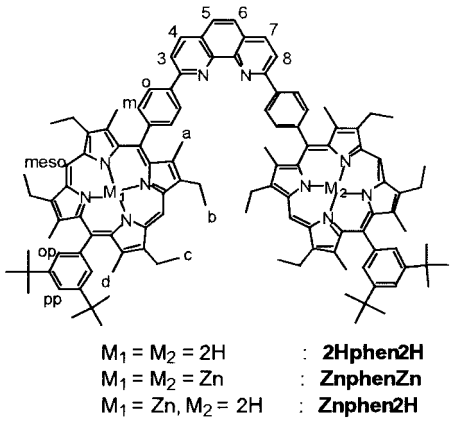

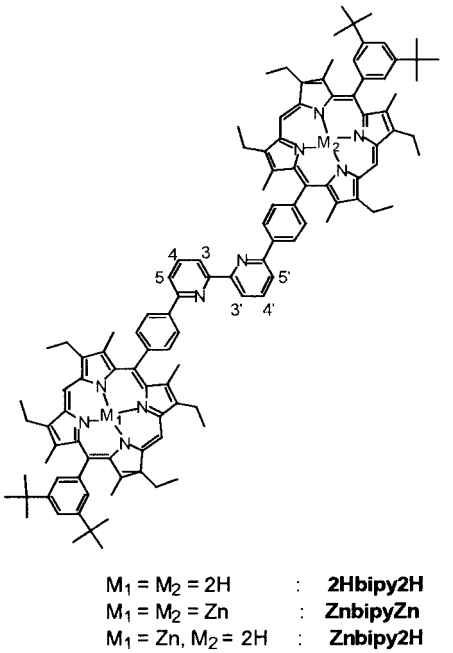

Figure 1. Molecular structures of 2Hphen2H, ZnphenZn, Znphen2H, 2Hbipy2H, ZnbipyZn, and Znbipy2H.

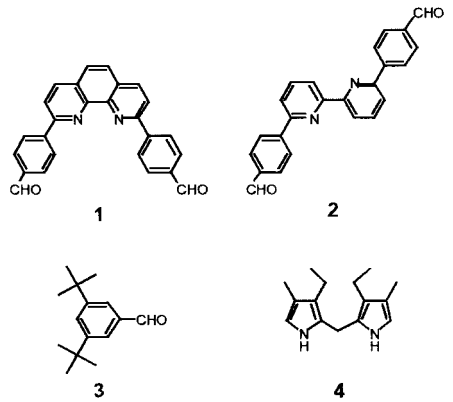

Figure 2. Molecular structures of the synthons **1**, **2**, **3**, **4**.

acid catalysis conditions, as described in detail below. 2,6-Di-(*p*-formylphenyl)-1,10-phenanthroline (**1**) was obtained as previously described.[9] The other dialdehyde precursor, 6,6′-di-(*p*-formylphenyl)-2,2′-bipyridine (**2**) was obtained as follows. The Grignard reagent of *p*-bromophenyl-1,3-dioxolane

0947-6539/99/0507-2090 $ 17.50+.50/0 *Chem. Eur. J.* **1999**, *5*, No. 7

(**6**) was prepared by metal exchange of *p*-lithiophenyl-1,3-dioxolane (obtained by reaction of **6** with *t*BuLi) with $MgBr_2$ (Figure 3). Pd-catalyzed cross-coupling of the organomagnesium reagent (1 equiv) with 2,6-dibromopyridine (**5**; 1 equiv) afforded 6-bromo-2-(*p*-phenyl-1,3-dioxolane)pyridine (**7**) in

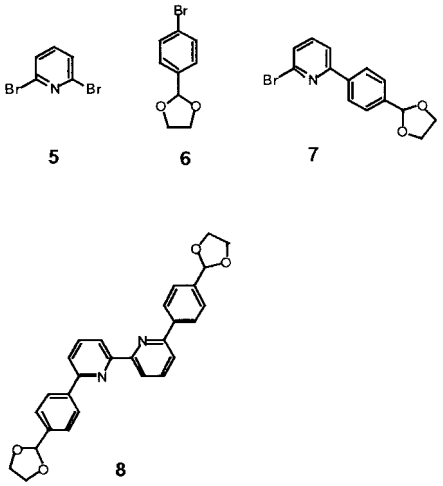

Figure 3. Molecular structures of the synthons **5**, **6**, **7**, **8**.

66% yield after chromatography. Subsequently, oxidative homocoupling[25] of 6-lithio-2-(*p*-phenyl-1,3-dioxolane)pyridine (2 equiv), obtained by reaction of *n*BuLi with **7**, in the presence of Cu^{II} (1 equiv) and oxygen, produced 6,6′-di-(*p*-phenyl-1,3-dioxolane)-2,2′-bipyridine (**8**) in 72% yield after chromatography. Compound **2** was finally obtained in 94% yield by hydrolysis of **8** with 5% HCl.

The target bis-porphyrin conjugates 2Hbipy2H and 2Hphen2H were obtained as follows: **2** was treated with 3,3′-diethyl-4,4′-dimethyl-2,2′-dipyrrylmethane (**4**;[26, 27] 10 equiv), 3,5-di-*tert*-butylbenzaldehyde (**3**;[9] 8 equiv), and five drops of trifluoroacetic acid at room temperature in CH_2Cl_2 for 17 h, following a procedure described by Lindsey et al.[28–30] Subsequently, a large excess of *p*-chloranil (40 equiv) was added to the intermediate porphyrinogens and the reaction mixture was heated to reflux for 2 h. After work up and chromatographic purification, bis-porphyrin 2Hbipy2H was obtained in 20% yield. Using the same reaction conditions and **1** as dialdehyde precursor, we obtaained dimer 2Hphen2H in nearly 15% yield after purification by column chromatography. The products were characterized by ^{1}H-NMR and FAB^+ mass spectrometry.

Typically, the FAB mass spectrum showed the molecular peak ($[M+H]^+$) and a peak corresponding to a species with a double positive charge ($[M+2H^+]/2$). The ^{1}H NMR spectrum of bis-porphyrin 2Hphen2H in $CDCl_3$ showed the expected signals, with the characteristic signatures of the meso protons at $\delta = 10.17$ and the NH protons at $\delta = -2.46$. In addition, the protons H_3 and H_4 (or H_8 and H_7) of the phenanthroline moieties produce a nice unusual AB pattern. For solubility reasons, the ^{1}H NMR spectrum of bis-porphyrin 2Hbipy2H was run in $CDCl_3$ containing a few drops of CF_3CO_2H. The spectrum is in agreement with the structure of the product; however, it cannot be directly compared with that of bis-porphyrin 2Hphen2H, because the peaks are broad and not well resolved.

The heterodimers Znphen2H and Znbipy2H cannot be obtained selectively. Reaction of $Zn(OAc)_2 \cdot 2H_2O$ (1 equiv) and the appropriate homodimer (2Hphen2H or 2Hbipy2H) in $CHCl_3$/MeOH (2:1) produced a mixture of bis-porphyrins: 2Hspacer2H, Znspacer2H, and ZnspacerZn, where spacer is either phen or bipy. The different porphyrin dimers were separated by column chromatography. In the bipy series, the distribution of products was 2Hbipy2H, 10%; Znbipy2H, 24%; ZnbipyZn, 32%; in the phen series, the distribution of products was 2Hphen2H, 18%; Znphen2H, 41%; ZnphenZn, 25%. In the latter case it was close to the statistical ratio of 25:50:25. In the former case, the statistics were not followed owing to solubility reasons: the ZnbipyZn dimer was more soluble than the 2Hbipy2H precursor and this increased the formation of ZnbipyZn at the expense of the heterodimer Znbipy2H. The compounds were characterized by FAB^+ mass spectrometry and by ^{1}H NMR spectroscopy in the case of the phen series. In the case of the bipy series, the poor solubility of the compounds in nonprotic solvents excluded analysis by ^{1}H NMR, since Zn^{II} incorporated in the porphyrins is removed by protonation. The data are in agreement with the metallation patterns. In particular, the NH resonances disappear upon metallation of the porphyrins with Zn^{II}. Otherwise, the metal has little or no influence on the chemical shifts of the other protons, either those belonging to the porphyrin or to the phenanthroline part of the molecule. The best diagnostic of metal incorporation into the tetrapyrrolic macrocycles is provided by UV/visible spectroscopy. This method is the best tool to follow the metallation reaction. The free-base compounds 2Hphen2H and 2Hbipy2H both show a Soret band around 410 nm (409 nm for 2Hphen2H and 412 nm for 2Hbipy2H) and four Q bands at 507, 540, 573, and 625 nm for 2Hphen2H, and 508, 541, 574, and 625 nm for 2Hbipy2H. As expected, upon incorporation of Zn^{II}, the four Q bands merge into one set of two bands, at 542 and 575 nm for ZnphenZn, and at 539 and 574 nm for ZnbipyZn. The spectra of the monometallated species Znphen2H and Znbipy2H are a superimposition of the spectra of the corresponding free-base and fully metallated species.

Structure calculations: Owing to the large number of atoms (253) it was not possible to use a semiempirical method that included solvent effects. Therefore we were limited to the Merck molecular force field. The conformation of minimum energy (Table 1) obtained for the *E* isomer of Znbipy2H was plausible and the distance between the centers of the two porphyrins amounted to 23 Å with a total strain energy of 945 kcal. However the van der Waals attraction between the porphyrin moieties led to a deformation of the N–C–phenyl valence angles of the *Z* isomers of Znbipy2H and Znphen2H compared with the values they had in the corresponding diphenylphenanthroline or 6,6′-diphenyl-2,2′-bipyridine. Furthermore a bending of the phenyl moieties over more than 10° occurred. This yielded an unrealistic short distance between the porphyrin centers of 8.15 Å and 8.24 Å in the *Z* isomers of Znbipy2H and Znphen2H, respectively. This van der Waals interaction is also suggested by the smaller strain energy

Table 1. Geometry and strain energies of Znbipy2H and Znphen2H.

	E [kcal]	R [nm]	θ_1 [°]	θ_2 [°]	φ_1 [°]	φ_2 [°]	φ_3 [°]	κ^2	$\langle\kappa^2\rangle$
Znbipy(Z)2H	113.10[a]		115.47[a]	116.10[a]	−22.07[a]	−23.05[a]	−23.05[a]		
	113.25[a]		115.52[a]	115.97[a]	−1.5[a]	−24.83[a]	−24.83[a]		
	937.1	8.15	113.9 ± 0.2	114.8 ± 0.15	−25.71	−49.52	−34.80	1.14 (0.94)	1.04
	937.1[b]	8.16	113.1 ± 0.3	114.2 ± 0.2	−20.77	−50.59	−37.90	0.80 (0.96)	0.87
	953.46[b]	15.36	115.46[c]	116.1[c]	56.04[d]	−19.93	−25.79	1.88 (0.27)	1.07
	940.24	8.21	115.42[c]	116.1[c]	−19.70[e]	−53.24	−37.95	1.14 (0.89)	1.04
Znbipy(E)2H	103.8[a]		115.58[a]	116.63[a]	175.50[a]	−33.27[a]	−33.27[a]		
	945.1	23.36	115.46 ± 0.02	116.62 ± 0.02	176.58	−32.02	−31.52	2.03 (2.71)	2.20
	945.0[b]	23.22	115.46 ± 0.02	116.4 ± 0.2	176.57	−32.16	−31.59	2.85 (2.42)	2.64
	945.2[b]	23.35	115.58[c]	116.65[c]	176.59	−32.37	−31.36	2.84 (2.19)	2.52
Znphen2H	133.27[f]		115.51[f]	118.47[f]	0.048[f]	−26.24[f]	−26.24[f]		
	967.3	8.24	112.9 ± 0.3	119.4 ± 0.2	−2.57	−63.97	−48.99	1.36 (1.32)	1.34
	978.3[b]	13.43	115.0 ± 0.05	120.77	−1.32	−27.71	−42.45	0.41 (1.93)	1.17
	976.37[b]	13.13	115.50[g]	118.47[g]	−1.30	−29.64	−40.53	1.35 (0.53)	0.94

[a] 6,6′-Diphenyl-2,2′bipyridine. [b] The phenyls are constrained to a planar geometry. [c] Constrained to the value in 6,6′-diphenyl-2,2′-bipyridine. [d] Starting from 20°. [e] Starting from −20°. [f] 1,10-diphenylphenanthroline. [g] Constrained to the value in 1,10-diphenylphenanthroline, θ_1: N−C−phenyl valence angle, θ_2: pyridyl−pyridyl−N valence angle, φ_1: dihedral angle between the two pyridyl moieties, φ_2: dihedral angle between a pyridyl moiety and the phenyl carrying H_2P, φ_3: dihedral angle between a pyridyl moiety and the phenyl carrying ZnP.

which amounted to 937 kcal in the Z isomer compared with 945 kcal in the E isomer. In Znphen2H the strain energy amounted to 967.3 kcal. Actually as a result of less extensive steric hindrance, a smaller strain energy would be expected for the E isomer compared with the Z isomer. The latter was confirmed for 6,6′-diphenyl-2,2′-bipyridine for which the Z isomer is 10.5 kcal above the E isomer. A more detailed study of the dependence of the energy of 2,2′-bipyridine or 6,6′-diphenyl-2,2′-bipyridine upon the dihedral angle shows that a small (1.0 kcal) maximum at the Z conformation is followed by a relatively wide plateau (up to 90°), at which the decrease of steric repulsion is largely balanced by a decrease of resonance energy. Only for larger values of the dihedral angle does the energy decrease steeply; this is caused by an increase of the resonance energy (negative) that is no longer compensated by an increase of repulsion energy (positive) to arrive eventually at the minimum 10.5 kcal below the Z conformer for a dihedral angle close to 180°. This corresponds to ab initio calculations[31, 32] for which differences of 6.9 and 9.5 kcal mol^{-1} were obtained between the *syn* and *anti* conformers of 2,2′-bipyridine. As only a STO-3G basis set was used in those calculations, those data can be rather inaccurate (cf. SPARTAN Manual). By means of electron diffraction measurements[33] a value of 5.6 kcal was obtained.

When the phenyl moieties are constrained to a planar geometry, the decreased van der Waals interaction increases the total strain energy and the center to center distance to 978 kcal and 13.43 Å, respectively, for Znphen2H, while for the Z and the E isomers of Znbipy2H both parameters remain the same when the geometry of the phenyl moieties was not constrained. Furthermore constraining the angles θ_1 and θ_2 (Figure 4) to the values they have in 6,6′-diphenyl-2,2′-bipyridine or 2,9-diphenyl-1,10-phenanthroline produces only marginal changes in the strain energy, the distance between the center of the porphyrins, and the dihedral angles in the E isomer of Znbipy2H and in Znphen2H. For the Z isomer of Znbipy2H no substantial changes are observed when a starting value of −20° is used for φ_1, the dihedral angle between the two pyridine planes. If, however, a starting value of +20° is used, the starting values for other bond angles and dihedral angles remaining the same, the distance between the centers of the porphyrins and the strain energy increase to 15.36 Å and 953.6 kcal, respectively. It should be mentioned that the dihedral angle of the bipy spacer (56°) resembles in the latter case that obtained by electron diffraction[33] for *cis*-2,2′-bipyridine (40°). The values obtained for θ_2 or $\sphericalangle C_2'C_2N$ (116.6°) correspond very well with those obtained from electron diffraction (116.1°).

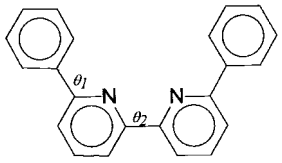

Figure 4. The bipyridyl moiety.

Steady-state measurements: The steady-state absorption and fluorescence spectra of the model compounds ZnP (P = porphyrin) and H_2P are displayed in Figure 5. Those of Znphen2H and Znbipy2H are displayed in Figures 6 and 7.

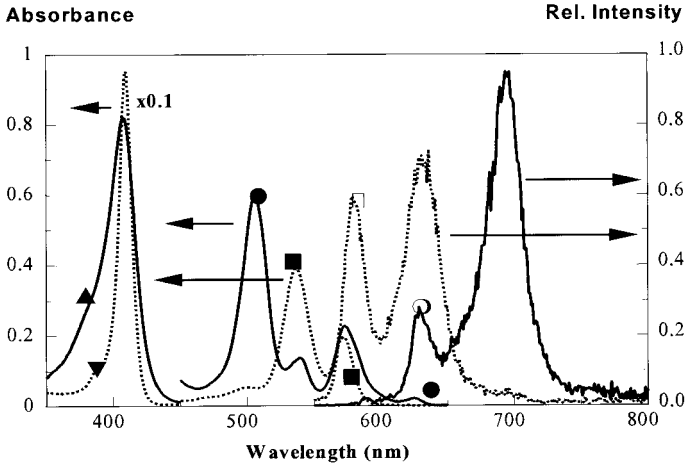

Figure 5. The steady-state absorption (■, ●) and emission (□, ○) spectra for the model compounds in dichloromethane; (- - -) ZnP, (—) H_2P. The emission spectra were obtained upon excitation at 540 nm. The absorption spectra of the Soret band (▼, ▲) were obtained in a 1 mm cuvette.

0947-6539/99/0507-2092 $ 17.50+.50/0 *Chem. Eur. J.* **1999**, *5*, No. 7

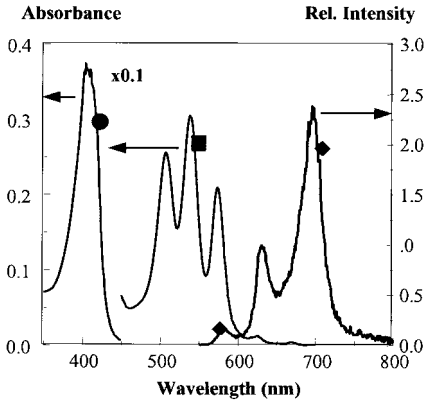

Figure 6. Absorption (■) and fluorescence (◆) spectra for Znphen2H in dichloromethane. The excitation wavelength for the fluorescence spectrum was 540 nm. The absorption spectrum of the Soret band was compressed 10 times (●).

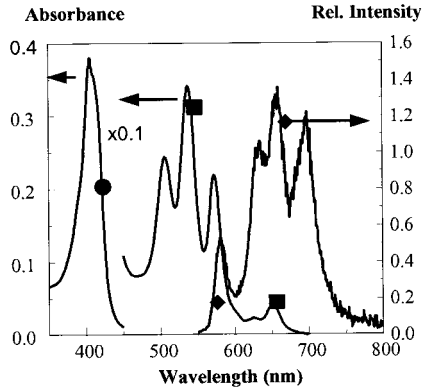

Figure 7. Absorption (■) and fluorescence (◆) spectra for Znbipy2H in dichloromethane. The excitation wavelength for the fluorescence spectrum was 540 nm. The absorption spectrum of the Soret band was compressed 10 times (●).

The absorption spectra of ZnP and H_2P are characterized by Q bands with maxima at 475, 501, 537, and 572, or 506, 540, 573, and 625 nm, respectively. The corresponding emission maxima are found at 579, 630, 695 and 627, 694, 750 nm. This means that the zero–zero transitions are situated at 2.15 eV for ZnP and 1.98 eV for H_2P. The fluorescence quantum yields of ZnP and H_2P in dichloromethane amount to 0.044 and 0.080, respectively.

The absorption spectrum of Znphen2H is characterized by maxima at 506 nm, 538 nm, 573 nm, 624 nm, and 648 nm (Figure 6). While the maxima at 506 and 624 nm can be attributed to the H_2P moiety, that at 538 nm is characteristic for the presence of the ZnP moiety. Also in the emission spectra, maxima at 578 nm and 633 nm (from the ZnP moiety) as well as maxima at 633 and 696 nm (from the H_2P emission) are observed.

The absorption spectrum of Znbipy2H (Figure 7) is characterized by maxima at 506 nm, 537 nm, 573 nm, 626 nm, and 651 nm. The maxima at 506 and 626 nm can be attributed to the H_2P moiety, while that at 538 nm is characteristic for the presence of the ZnP moiety. Similarly the emission spectrum has maxima at 580 nm and 632 nm, due to the ZnP moiety, and at 632 and 698 nm, which relates to emission of H_2P. Furthermore a maximum at 657 nm is observed which does not relate to maxima obtained for the model compounds.

At wavelengths below 600 nm the absorption spectra of these compounds appear to be essentially a superposition of those of the model compounds. However, it should be noted that for Znbipy2H (and to a smaller extent for Znphen2H) a small band near 650 nm is also present, as is an extra band in the emission spectrum centered at 657 nm. The emission spectrum of Znphen2H is nearly identical to that of H_2P, while that of Znbipy2H still shows an important contribution of ZnP emission. The excitation spectrum for Znbipy2H was recorded at several emission wavelengths (see Figure 8) and

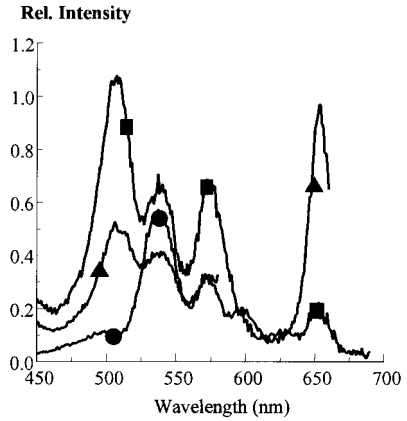

Figure 8. The excitation spectrum of Znbipy2H monitored at different emission wavelengths; (●): 582 nm, (▲): 665 nm, (■): 695 nm.

confirmed the presence of what we suspect is a fluorescing impurity in Znbipy2H; this is evident when monitoring the emission at 665 nm and to a lesser extent at 695 nm. Otherwise Figure 8 shows that at the emission wavelength of 582 nm the excitation spectrum is similar to the absorption spectrum of ZnP, that is, the fluorescence originates from the zinc porphyrin. At longer monitoring wavelengths the spectrum is similar to the absorption spectrum of H_2P. The exception to this is the size of the impurity band, which is more intense in the excitation spectrum, indicating a high fluorescent quantum yield. The presence of an impurity in these compounds is not completely unexpected because of the complexity of the synthesis and purification process. In this case the existence of such an impurity was easily noticed from both the absorption and emission spectra and so can be borne in mind when analyzing the time-resolved data.

The fluorescence spectra of Znbipy2H and Znphen2H show the principal emission from ZnP to be at 582 nm and 630 nm, while that from H_2P is at 630 nm and 695 nm. Upon excitation at 540 nm (chosen as at this wavelength a majority ca. 76% of the incident light would be absorbed by the zinc porphyrin) the fluorescence spectra from the bridged compounds (Figures 6 and 7) show that the zinc-porphyrin fluorescence at 582 nm is quenched relative to that of the model compound. The quantum yields for the emission of ZnP in the two bridged systems were found to be 0.015 and 0.007. As one would expect the quenching is greatest in Znphen2H, in which the distance between the two porphyrin subunits is smaller. The center to center distances between the two porphyrin moieties were estimated to be about 23 Å for Znbipy2H and 13 Å for Znphen2H. The stationary fluores-

cence spectra suggest that the main effect on the fluorescence intensity and lifetime should be evident at 582 nm, at which the fluorescence emission should emanate solely from the zinc porphyrin.

Time-resolved fluorescence

Znphen2H: The fluorescence decays of ZnP and H_2P could be analyzed as a single exponential decay that yield decay times of 1.31 ± 0.01 ns and 9.72 ± 0.01 ns, respectively. Individual decays of the fluorescence of Znphen2H (Figure 9) could be

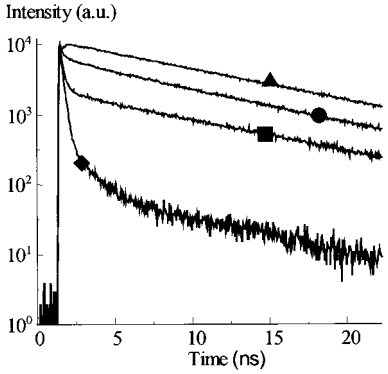

Figure 9. Fluorescence decays of Znphen2H. The time increment was 0.0437 ns per channel. Excitation occurred at 540 nm (◆), at 582nm, (■) at 630 nm, (●) at 665 nm, and (▲) at 695 nm.

analyzed as a sum of three exponentials [Eq. (1)] that yields a fast decay time between 0.11 and 0.16 ns, a slow decay time between 8.2 and 11.1 ns, and an intermediate decay time between 0.95 and 1.25 ns (for decays at 582, 630, and 695 nm).

$$I(t) = A_1 \exp^{-\lambda_1 t} + A_2 \exp^{-\lambda_2 t} + A_3 \exp^{-\lambda_3 t} \quad (1)$$

$$I(t) = A_1 \exp^{-\lambda_1 t} + A_2 \exp^{-\lambda_2 t} + A_3 \exp^{-\lambda_3 t} + A_4 \exp^{-\lambda_4 t} \quad (2)$$

In Equation (1) λ_1, λ_2, and λ_3 (ns^{-1}) correspond to the three inverse decay times and A_1, A_2, and A_3 to the relative amplitudes immediately after excitation by a δ pulse. At 665 nm values between 1.37 and 1.58 ns are observed for the intermediate decay time. The fast decaying component prevails at 582 nm, but its contribution becomes negative at 695 nm. The slow decaying component (which has a negligible contribution at 582 nm) becomes more prevalent at 665 and 695 nm.

Global analysis of the fluorescence decays at 582, 630, 665, and 695 nm as a sum of three exponentials, yields decay times of 0.16, 1.26, and 9.71 ns ($\chi_g^2 = 1.09$). As the second and third decay time were very close to those obtained for ZnP and H_2P respectively an attempt to link the decays of ZnP and H_2P to those of Znphen2H was made. Here a four exponential decay model [Eq. (2)] only produced a marginal fit ($\chi_g^2 = 1.26$) to the data.

In Equation (2) λ_1, λ_2, λ_3, and λ_4 (ns^{-1}) correspond to the inverse decay times and A_1, A_2, A_3, and A_4 to the relative amplitudes immediately after excitation by a δ pulse. However, by excluding the decay at 665 nm a very good fit as a sum of three exponentials (Table 2) was obtained. This confirms that, as already suggested by the stationary emission spectrum

Table 2. Fluorescence decay parameters of Znphen2H obtained by global analysis as a sum of three exponentials; λ_2 and λ_3 were linked to the fluorescence decay rates of ZnP and H_2P, respectively; $\chi_g^2 = 1.06$.

	582 nm[a]	582 nm[b]	630 nm[b]	695 nm[b]
A_1	0.93 ± 0.01	0.97 ± 0.02	0.85 ± 0.02	-0.432 ± 0.008
λ_1 [ns^{-1}]	6.48 ± 0.21	6.48 ± 0.21	6.48 ± 0.21	6.48 ± 0.21
A_2	0.061 ± 0.001	0.024 ± 0.001	0.025 ± 0.002	0.025 ± 0.005
λ_2 [ns^{-1}]	0.758 ± 0.006	0.758 ± 0.006	0.758 ± 0.006	0.758 ± 0.006
A_3	0.0051 ± 0.0001	0.0041 ± 0.0001	0.126 ± 0.0016	0.975 ± 0.015
λ_3 [ns^{-1}]	0.1025 ± 0.0007	0.1025 ± 0.0007	0.1025 ± 0.0007	0.1025 ± 0.0007
$\bar{c}_2$[c]	0.0058	0.0044	0.12	0.68
$\bar{c}_2$[d]	~ 0	~ 0	0.096	0.74
χ^2	1.13	0.98	1.05	1.18

[a] Time increment per channel 0.0219 ns. [b] Time increment per channel 0.0437 ns. [c] Irreversible energy transfer. [d] Reversible energy transfer.

of Znbipy2H, emission of another molecule other than a monomer of Znphen2H is observed at 665 nm. Also it should be noted that the amplitude of the component with a decay time of 0.17 ns, which has overwhelming amplitude at 582 nm, becomes negative at 695 nm. On the other hand the 9.7 ns component, which has negligible amplitude at 582 nm, becomes the major one at 695 nm. If the decay at 665 nm is included in the analysis a fourth component with a decay time of 3.3 ns and zero amplitude at 582 nm is necessary. In this case the amplitude A_2 becomes negligible at 695 nm.

As the excitation and emission spectra suggest that an energy-transfer process is occurring, the analysis of the fluorescence decays will be considered in this framework. The simplest kinetic scheme for the energy transfer can be given in Scheme 1. In Scheme 1, k_{21} corresponds to the rate constant for energy transfer between ZnP and H_2P, while k_{01} and k_{02} correspond to the sum of the rate constants of the radiative and radiationless decay processes of the ZnP and H_2P moieties, respectively. β_1 and β_2 give the fraction of the excitation absorbed by both the zinc and the metal-free porphyrins with $\beta_1 + \beta_2 = 1$. This scheme yields a monoexponential decay with decay rate $k_{01} + k_{21}$ for the ZnP moiety and a biexponential decay with decay rates $k_{01} + k_{21}$ and k_{02} for the H_2P-moiety. Taking into account the wavelength dependence of the preexponential factors, the component $A_1 \exp\text{-}\lambda_1 t$ should correspond to the emission of ZnP at short wavelengths, while the component $A_3 \exp^{-\lambda_3 t}$ should correspond to that of H_2P. The component $A_2 \exp^{-\lambda_2 t}$ is attributed to ZnP moieties that are unable to transfer energy. The small value of A_2 at all wavelengths makes it impossible to assign this component more precisely. The ratio of the preexponential factors A_3/A_1 will depend upon β_1 and the ratio $k_{21}/(k_{01} + k_{21} - k_{02})$. In this framework the ratio A_3/A_1 should equal -1.28 at 695 nm. Experimentally a value of -2.26 is observed at 695 nm. This suggests that even at 695 nm the emission of ZnP still overlaps with that of H_2P. If the fluorescent rate constant of ZnP and H_2P at wavelength λ_{em} are given by $c_1(\lambda_{em})$ and $c_2(\lambda_{em})$[34–36] the observed fluorescence decay will be given by Equations (3) – (5).

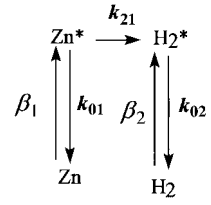

Scheme 1.

0947-6539/99/0507-2094 $ 17.50+.50/0 *Chem. Eur. J.* **1999**, *5*, No. 7

$$I(t) = I_{abs}[(\bar{c_1}\beta_1 - \bar{c_2}\beta_1\gamma)\exp^{-(k_{21}+k_{01})t} + (\bar{c_2}\beta_2 + \bar{c_2}\beta_1\gamma)\exp^{-k_{02}t} \quad (3)$$

$$k_{f1} = \int c_1(\lambda_{em})d\lambda_{em} \quad (4a)$$

$$k_{f1} = \int c_2(\lambda_{em})d\lambda_{em} \quad (4b)$$

$$\bar{c_1} = \frac{c_1}{c_1 + c_2} \quad (5a)$$

$$\bar{c_2} = \frac{c_2}{c_1 + c_2} \quad (5b)$$

$$\gamma = \frac{k_{21}}{k_{21} + k_{01} - k_{02}} \quad (5c)$$

This yields values for $\bar{c_2}$ at 630 and 695 nm of 0.12 and 0.68, respectively, while k_{21} and k_{02} equal $5.72 \times 10^9\,s^{-1}$ and $1.03 \times 10^8\,s^{-1}$, respectively, (Table 3) From the spectral data and the

Table 3. Kinetic parameters of Znphen2H.

	Scheme 1	Scheme 2
k_{01} [ns^{-1}]	0.758 ± 0.006	0.758 ± 0.006
k_{21} [ns^{-1}]	5.72 ± 0.22	5.69 ± 0.22
k_{12} [ns^{-1}]	–	$0.024 \pm .018$
k_{02} [ns^{-1}]	0.1026 ± 0.0007	$0.101 \pm .025$

values of k_{f1} and k_{f2}, values of 0.075 and 0.86 are obtained for $\bar{c_2}$ at 630 nm and 695 nm. The value of 0.0044 obtained for $\bar{c_2}$ at 582 nm can be related to the spectral overlap; however, a reversible energy transfer between the ZnP and the H_2P moieties could also yield the same result. Although in this case at all wavelengths the fluorescence decays remain biexpotential the expressions for the preexponential factors become more complicated in the framework of Scheme 2.

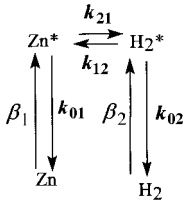

Scheme 2.

$$I(t) = I_{abs}\{[\bar{c_1}(\beta_1\gamma_{11} - \beta_2\gamma_1) + \bar{c_2}(\beta_2\gamma_{12} - \beta_1\gamma_2)]\exp^{-\lambda_1 t} + [\bar{c_1}(\beta_1\gamma_{12} + \beta_2\gamma_1) + \bar{c_2}(\beta_1\gamma_2 + \beta_2\gamma_{11})]\exp^{-\lambda_3 t}\} \quad (6)$$

$$\lambda_{1,3} = \frac{X + Y \pm \sqrt{[(X-Y)^2 + 4k_{12}k_{21}]}}{2} \quad (7)$$

$$X = k_{01} + k_{21} \quad (8a)$$

$$Y = k_{02} + k_{12} \quad (8b)$$

$$\gamma_{11} = \frac{\lambda_1 - Y}{\lambda_1 - \lambda_3} \quad (9a)$$

$$\gamma_{12} = \frac{Y - \lambda_3}{\lambda_1 - \lambda_3} \quad (9b)$$

$$\gamma_1 = \frac{Y - k_{02}}{\lambda_1 - \lambda_3} \quad (9c)$$

$$\gamma_2 = \frac{X - k_{01}}{\lambda_1 - \lambda_3} \quad (9d)$$

While k_{01} is known from the model compound ZnP and β_1 is known from the absorption spectra, one can calculate k_{12} and k_{21} from the decay rates and preexponential factors if one assumes that $\bar{c_2} = 0$ at 582 nm. This yields $5.69 \times 10^9\,s^{-1}$, $2.4 \times 10^7\,s^{-1}$, and $1.01 \times 10^8\,s^{-1}$ for k_{21}, k_{12}, and k_{02}, respectively. When the data are analyzed in this framework (assuming $\bar{c_2} = 0$ at 582 nm) values of 0.096 and 0.74 are obtained for $\bar{c_2}$ at 630 and 695 nm, respectively. Allowing the energy transfer to be reversible leads to a small decrease of k_{02} and a small increase of $\bar{c_2}$ at 695 nm. The changes of k_{21} and of $\bar{c_2}$ at 630 and 695 nm are marginal. This is no surprise, as k_{12} remains always significantly smaller than k_{21} or k_{02}. From the ratio of k_{21}/k_{12} a free energy difference between the singlet excited states of ZnP and H_2P of -0.13 eV could be determined. This is close to the spectroscopic energy difference of -0.17 eV. If both spectral overlap and reversible energy transfer occur, values of k_{12} between zero and $2.4 \times 10^7\,s^{-1}$ should be found, while $\bar{c_2}$ at 582 nm must be positive but smaller than 0.0044. In the frameworks of Schemes 1 or 2 the fluorescent quantum yield of the ZnP moiety in Znphen2H, φ_{f1} is given by Equation(10). This would yield a value of 0.0065, which is very close to the experimental value of 0.007.

$$\varphi_{f1} = k_{f1}\left(\frac{A_1\,(582\,nm)}{\lambda_1} + \frac{A_3\,(582\,nm)}{\lambda_3}\right) \quad (10)$$

Znbipy2H: In analogy to the observations made for Znphen2H the fluorescence decays of Znphen2H at 582 and 630 nm (Figure 10) could be analyzed as a sum of three

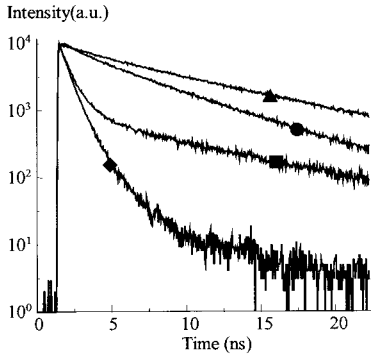

Figure 10. Fluorescence decays of Znbipy2H. The time increment was 0.0437 ns per channel. Excitation occurred at 540 nm (◆), at 582nm, (■) at 630 nm, (●) at 665 nm, and (▲) at 695 nm.

exponentials. Here the shortest decay time lengthened from 0.2 to 1.1 ns upon increasing the wavelength, while the intermediate and longest decay times increased from 0.6 to 4.8 and from 1.9 to 10.7 ns, respectively. This suggests that in this case the fluorescence decay is more complex. A global analysis, even as a sum of four exponentials, yielded only satisfactory statistical parameters when the decay at 665 nm (Figure 10) was omitted. Under those conditions global decay times of 0.24, 0.699, 1.61, and 9.04 ns were obtained. As the two longer decay times are relatively close to those of ZnP and H_2P again, an attempt was made to include the decays of the two model compounds in the global analyses. This four exponential global analysis led to acceptable statistical parameters when one of the decay times of the decay at 695 nm (Figure 10) was not linked. The decay parameters show that while decay is at short wavelengths governed by a component with a decay time of 0.56 ns, at longer wavelengths the component with a decay time of 9.75 ns prevails. The amplitude of the component with a decay time of 83 ps is 30 % of that of the component with a decay time of 0.56 ns at 582 and 630 nm. As the fastest decay rate is characterized by a very large standard deviation an attempt to fix the latter to the fast decay rate of Znphen2H was made. This led only to a marginal increase of χ^2_g (Table 4b) and to minor changes of the amplitudes of the relative components.

Table 4. Fluorescence decay parameters of Znbipy2H obtained by global analysis as a sum of three exponentials, λ_3 and λ_4 were linked to the fluorescence decay rates of ZnP and H_2P, respectively. a) λ_1 was allowed to float, $\chi^2_g = 1.10$; b) λ_2 was fixed to the fast decay rate of Znphen2H, $\chi^2_g = 1.11$.

	582 nm[a]	582 nm[b]	630 nm[b]	695 nm[b]
a)				
A_1	0.14 ± 0.02	0.22 ± 0.04	0.27 ± 0.05	0.34 ± 0.02
λ_1 [ns^{-1}]	12.0 ± 6.9	12.0 ± 6.9	12.0 ± 6.9	12.0 ± 6.9
A_2	0.66 ± 0.02	0.65 ± 0.03	0.52 ± 0.025	0.032 ± 0.005
λ_2 [ns^{-1}]	1.78 ± 0.08	1.78 ± 0.08	1.78 ± 0.08	1.78 ± 0.08
A_3	0.196 ± 0.007	0.132 ± 0.007	0.15 ± 0.01	0.032 ± 0.012
λ_3 [ns^{-1}]	0.758 ± 0.005	0.758 ± 0.005	0.758 ± 0.005	0.281 ± 0.007
A_4	0.0020 ± 0.0001	0.0016 ± 0.0001	0.054 ± 0.003	0.44 ± 0.02
λ_4 [ns^{-1}]	0.102 ± 0.001	0.102 ± 0.001	0.102 ± 0.001	0.102 ± 0.001
$\bar{c}_2$	0.0023	0.0021	0.062	0.59
χ^2	1.05	0.98	1.24	1.23
b)				
A_1	0.135 ± 0.005	0.21 ± 0.01	0.23 ± 0.01	0.27 ± 0.02
λ_1 [ns^{-1}]	6.48	6.48	6.48	6.48
A_2	0.66 ± 0.08	0.66 ± 0.07	0.54 ± 0.07	-0.01 ± 0.02
λ_2 [ns^{-1}]	1.72 ± 0.09	1.72 ± 0.09	1.72 ± 0.09	1.72 ± 0.09
A_3	0.200 ± 0.007	0.136 ± 0.006	0.17 ± 0.01	0.22 ± 0.012
λ_3 [ns^{-1}]	0.758 ± 0.005	0.758 ± 0.005	0.758 ± 0.005	0.290 ± 0.008
A_4	0.0021 ± 0.0001	0.0018 ± 0.0001	0.059 ± 0.01	0.51 ± 0.02
λ_4 [ns^{-1}]	0.1026 ± 0.0010	0.1026 ± 0.0010	0.1026 ± 0.0010	0.1026 ± 0.0010
$\bar{c}_2$	0.0026	0.0024	0.083	0.64
χ^2	1.03	1.01	1.23	1.30

[a] Time increment per channel 0.0219 ns. [b] Time increment per channel 0.0437 ns.

In the framework of Scheme 1 or Scheme 2 (with $k_{12} \ll k_{21}$) the component $A_2 \exp^{-\lambda_2 t}$, characterized by a large amplitude at 582 nm and a very small (Table 4a) or negative amplitude (Table 4b) at 695 nm, can be attributed to ZnP emission at 582 nm (short wavelengths). The component $A_4 \exp^{-\lambda_4 t}$ must be attributed to emission of H_2P. The component $A_3 \exp^{-\lambda_3 t}$ should be attributed to ZnP moieties, which are unable to transfer energy. As the component $A_1 \exp^{-\lambda_1 t}$ has an important amplitude, this suggests that the kinetics for Znbipy2H are clearly more complex than for Znphen2H. As the bipy bridge is more flexible than the phen bridge, this component could be associated with a conformation in which energy transfer is more efficient than in the predominant E conformer of the bipy bridge, with which the component $A_2 \exp^{-\lambda_2 t}$ is associated. Attributing the short decay time (0.56 or 0.70 ns) with the largest contribution to the E configuration of the bipy bridge makes sense, as the distance between donor and acceptor is longer than in Znphen2H (23.2 versus 14.2 Å). The short decay time was obtained less accurately and corresponds within the experimental uncertainty to the short decay time observed for Znphen2H. This could be related to a Z configuration of the bipy bridge. When the fractions of the two conformers are given by α_F and $\alpha_S (\alpha_F + \alpha_S = 1)$, the kinetic scheme can be proposed for irreversible energy transfer (Scheme 3) yielding the decay given by Equation (11). γ_F and γ_S are defined in Equations (12a) and (12b); all other parameters have the same meaning as for Znphen2H.

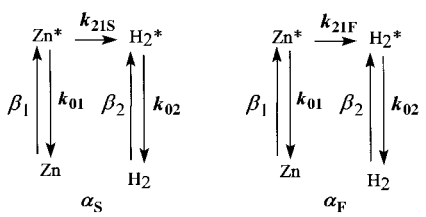

Scheme 3.

$$I(t) = I_{abs}[\alpha_S \beta_1 (\bar{c_1} - \bar{c_2}\gamma_S) \exp^{-\lambda_2 t} + \alpha_F \beta_1 (\bar{c_1} - \bar{c_2}\gamma_F) \exp^{-\lambda_1 t} + \bar{c_2}[\beta_2 + \beta_1(\alpha_S \gamma_S + \alpha_F \gamma_F)] \exp^{-\lambda_4 t} \quad (11)$$

$$\gamma_F = \frac{\lambda_1 - k_{01}}{\lambda_1 - \lambda_4} \quad (12a)$$

$$\gamma_S = \frac{\lambda_2 - k_{01}}{\lambda_2 - \lambda_4} \quad (12b)$$

From the ratios of the preexponentials A_2/A_1, values of 0.74 and 0.24 are obtained for α_S and α_F. $\bar{c_2}$ can be calculated from the ratio of the preexponential factors of $\exp(-\lambda_1 t)$ and $\exp(-\lambda_4 t)$ or that of $\exp(-\lambda_2 t)$ and $\exp(-\lambda_4 t)$. As the latter preexponential factors and decay times could be determined more accurately these were preferred. While at 582 and 630 nm both approaches led to similar values for $\bar{c_2}$, a considerably smaller value was obtained for $\bar{c_2}$ at 695 nm when the fast component was used. With the slow components, the values of $\bar{c_2}$ were slightly smaller (Table 4a) at the different analysis wavelengths than those obtained for Znphen2H (Table 2).

In principle the energy transfer could also be reversible for Znbipy2H. In this case a numerical analysis of the data becomes impossible, and therefore this combination was not explored. However, one should take into account that for Znphen2H allowing the energy transfer to be reversible led only to minimal changes of k_{21}, k_{02}, and $\bar{c_2}$; hence one can assume that the data obtained for Znbipy2H remain reliable. This will, a fortiori, be the case in Znbipy2H in which k_{21S} is much smaller than the value obtained for k_{21} in Znphen2H.

If the fast decaying component at 582 nm is due to a Z conformation of the bipy bridge, its decay time should be close to the decay time of the ZnP moiety in Znphen2H and the distance between and relative orientation of ZnP and H_2P should be similar in both molecules. As the fast decay time (λ) is characterized by a large experimental error an attempt was made to analyze the decays by fixing λ to the value obtained for Znphen2H. As this procedure yielded a good fit with the experimental data, we performed a further analysis of the decay parameters given in Table 4b and obtained the rate constants and fractions given in the right-hand column of Table 5. Here it can be seen that the values of $\bar{c_2}$ are found to be larger for all wavelengths. Thus the values approach those obtained from k_{f1}, k_{f2}, and the spectral features. However, use of either the data in Table 4a or Table 4b led to insignificant changes in the other parameters (k_{21S}, k_{02}, α_S, α_F).

In the framework of Scheme 3 the fluorescent quantum yield of the ZnP moiety in Znbipy2H, φ_{f1} is given by

Table 5. Kinetic parameters of Znbipy2H determined by interpretation of the fluorescence decays in the framework of Scheme 3.

	λ_1 floating	$\lambda_1 = 6.48 \times 10^9$ s^{-1}
k_{01} [ns^{-1}]	0.758 ± 0.005	0.758 ± 0.005
k_{21S} [ns^{-1}]	1.0 ± 0.09	0.96 ± 0.1
k_{21F} [ns^{-1}]	12.0 ± 7	5.72 ± 0.25
k_{02} [ns^{-1}]	0.102 ± 0.001	0.103 ± 0.001
α_S	0.74 ± 0.03	0.80 ± 0.05
α_F	0.26 ± 0.03	0.20 ± 0.05

0947-6539/99/0507-2096 $ 17.50+.50/0 Chem. Eur. J. 1999, 5, No. 7

Equation (13). This would yield a value of 0.014, which is within the experimental error from the value of 0.015 determined from the stationary fluorescence data.

$$\varphi_{fl} = k_{fl}\left(\frac{A_1\,(582\,\mathrm{nm})}{\lambda_1} + \frac{A_2\,(582\,\mathrm{nm})}{\lambda_2}\right) \tag{13}$$

Combining the fluorescence decays and stationary-fluorescence and absorption spectra suggests that the photophysics of Znphen2H and Znbipy2H can be described by a combination of monomolecular decay processes, which occur with the same rate as in the model compounds, and energy transfer. It is difficult to conclude from the data whether the energy transfer is reversible as suggested by the singlet energies.

Depending upon the assumptions used, the ratio α_F/α_S obtained from the analysis of the fluorescence decays of Znbipy2H suggests that the *E* conformer is 620 or 820 cal mol^{-1} (ΔG°) more stable than the *Z* conformer. This difference is an order of magnitude below the values obtained for 2,2′-bipyridine by ab initio calculations[31, 32] or electron diffraction.[33] One should consider that the latter values were obtained for the gas phase and that in solution (especially in a polar solvent as dichloromethane) the *Z* conformer can be better solvated than the *E* conformer;[37, 38] this decreases the free-energy difference to, for example, 2.03 kcal in *n*-hexane and 1.17 kcal in $CHCl_3$.

The rate constant for energy transfer: In a qualitative way the larger value of k_{21}, determined in Znphen2H compared with k_{21S}, determined in Znbipy2H corresponds to a larger distance between the center of the two porphyrins. However, in the framework of Förster transfer ($k \sim R^{-6}$) the ratio of both rate constants should amount to 31.6, while both stationary and time-resolved experiments suggest only a value of 5.95.

Therefore we have attempted to evaluate both rate constants directly from data of spectral overlap, the absorption spectrum of H_2P and the fluorescence rate constant of ZnP, and the geometric data obtained by the molecular mechanics calculations [Eq. (14)].

$$k_{21} = \frac{9000\langle\kappa\rangle^2(\ln 10)k_{fD}}{128\pi^5 n^4 N_A R^6}\int\frac{\varepsilon_A(\nu)f_D(\nu)\mathrm{d}\nu}{\nu^4\int f_D(\nu)\mathrm{d}\nu} + \frac{9000\langle\kappa\rangle^2(\ln 10)k_{fD}}{128\pi^5 n^4 N_A R^6}\int\frac{\varepsilon_A(\lambda)f_D(\lambda)\lambda^6\mathrm{d}\lambda}{\int f_D(\lambda)\lambda^2\mathrm{d}\lambda} \tag{14}$$

In this equation $\varepsilon_A(\lambda)$ or $\varepsilon_A(\bar{\nu})$ [l mol^{-1} cm^{-1}] is the molar extinction coefficient of the acceptor, $f_D(\lambda)$ (nm^{-1}) or $f_D(\bar{\nu})$ [nm] is the fluorescence spectrum of the donor, *n* is refractive index of the solution (1.42 for dichloromethane), N_A is Avogadro's number, k_{fD} is the fluorescent rate constant of the donor (3.359×10^7 s^{-1}), *R* [nm] is the distance between donor and acceptor, and $\langle\kappa\rangle^2$ is an orientation factor. According to Mårtensson[39] $\langle\kappa\rangle^2$ rather than $\langle\kappa^2\rangle$ should be used for energy transfer between a doubly degenerated (ZnP) and a non-degenerated (H_2P) excited state. By using the averaging procedure developed by Mårtensson we obtain a value for Znphen2H of 1.35 and 0.53 for both possible orientations of the transition dipole of H_2P. When a fast interconversion between both isomers is observed an average value of 0.94 should be used for $\langle\kappa^2\rangle$. In the same way we obtain values of 2.84 and 2.42 for both orientations of the transition dipole of H_2P in the *E* isomer of Znbipy2H, while for the *Z* isomer we obtain 1.88 and 0.27. This leads to average values of 2.64 and 1.07 for the *E* and *Z* isomer, respectively. From Equation (14) a value of 2.8×10^{10} s^{-1} is found for k_{21} in Znphen2H. For the *Z* conformer of Znbipy2H a value of 1.4×10^{10} s^{-1} (6.3×10^{11} s^{-1} with a center-to-center distance of 8.16 Å) is found for k_{21F}. For the *E* conformer of Znbipy2H a value of 2.8×10^9 s^{-1} is obtained for k_{21S}. When those values are compared with the values obtained from the fluorescence decays we see that k_{21} is always overestimated, ranging from a factor 2 in the *E* isomer of Znbipy2H to a factor 5 in Znphen2H. For the *Z* isomer of Znbipy2H, k_{21} is calculated correctly or overestimated by a factor 15 to 20 depending on which geometry is preferred. This discrepancy can have several causes.

One possibility is that for chromophores whose dimensions approach the distance between their centers the Coulomb interaction can no longer be reduced to a simple dipole–dipole interaction. It has been shown by Czikelly[40, 41] and Norland[42] that this effect will overestimate the interaction and that the error becomes relatively more important when the center-to-center distance becomes smaller. For example, while the exciton splitting of the excited state of a sandwich pair of cyanine molecules is overestimated by a factor of 7 for a separation of 6 Å, this reduces to a factor of 4 and 3 at an intermolecular distance of 8 and 10 Å, respectively. Also in a monopole model Chang[43] obtains for a coplanar arrangement of two chlorophylls, as in the *Z* isomer of Znbipy2H and Znphen2H, a matrix element for the Coulomb interaction that is at a separation of 10 Å about 50% smaller than the matrix element calculated on the basis of a Coulomb interaction between two point dipoles. This would reduce k_{21} by a factor of 4. For the *E* isomer of Znbipy2H the situation is more complex: while for two coplanar chlorophylls the matrix element is increased for parallel transition dipoles oriented along the intermolecular axis, it is decreased for transition dipoles perpendicular to the intermolecular axis.

A second possibility is that the energy transfer is not purely driven by Coulomb interaction, but that configuration interaction with charge-transfer configurations[44–46] as well exchange interactions[47] also provides a contribution to the rate constant for energy transfer. This contribution, which will be largely through-bond,[45,48,49] will not be very different for Znphen2H and the *E* isomer of Znbipy2H. However, in the latter case one expects (unless some interference effects occur) that theoretical models would underestimate rather than overestimate k_{21}.

Conclusion

While both porphyrin dimers show the same topology (substitution meta to the bond between the two pyridyl moieties[50, 51]), a large difference of the rate of energy transfer is observed between Znphen2H and the major conformer of Znbipy2H. This suggests that the energy transfer is mainly through space and probably is due to a Coulomb mechanism. As the size of the chromophores is not negligible compared with their center-to-center distance, it is no surprise that reducing the Coulomb interaction to a point-dipole model

overestimates[40–43] the rate of energy transfer, especially for Znphen2H and the *Z* conformer of Znbipy2H.

The detailed analysis of the fluorescence decays suggests furthermore that about 30% of Znbipy2H is present in the less-stable *Z* conformer. When it is assumed that the slow-decaying component of the fluorescence of Znphen2H at 582 nm is due to a reversible energy transfer, the ratio of the forward and backward energy-transfer steps matches the free-energy difference between the excited state of the zinc porphyrin and the metal-free porphyrins as suggested by the position of the 0–0 transitions. For the major (*E*) conformer of Znbipy2H, which is characterized by a three times slower forward energy transfer and a similar free-energy difference between both singlet excited states, the rate of the backward transfer is so small that it does not yield values of $\tilde{c}_2$ that differ appreciably from zero.

Experimental Section

Synthesis: Dialdehyde **1**,[9] 3,5-di-*tert*-butylbenzaldehyde (**3**),[9] 3,3′-diethyl-4,4′-dimethyl-2,2′-dipyrrylmethane (**4**),[26, 27] and *p*-bromophenyl-1,3-dioxolane (**6**) were prepared according to the literature procedures. All other chemicals were of the best commercially available grade and were used without further purification. Dry solvents were obtained by distillation from P_2O_5 (CH_2Cl_2) or Na/benzophenone (Et_2O and THF). UV/visible spectra were recorded on a Kontron Instruments UVIKON 860 spectrophotometer. ^{1}H NMR spectra were recorded on Bruker WP200SY spectrometer. Fast atom bombardment mass spectra (FAB-MS) were obtained in the positive-ion mode with either a krypton primary atom beam in conjunction with a 3-nitrobenzyl alcohol matrix and a Kratos MS80RF mass spectrometer coupled to a DS90 system or a xenon primary atom beam with the same matrix and a ZAB-HF mass spectrometer.

6-Bromo-2-(*p*-phenyl-1,3-dioxolane)pyridine (7): A solution of *tert*-butyllithium in pentane (1.4 M, 32.2 mL, 43.7 mmol) was added to a solution of *p*-bromophenyl-1,3-dioxolane **6** (5.00 g, 21.8 mmol) in THF (100 mL) at −98 °C under argon and was stirred for 10 min at this temperature. Then a saturated solution of $MgBr_2$ (2.62 M; prepared from 2.43 g of Mg and 8.9 mL of dibromoethane in 50 mL of Et_2O) was added, and the mixture was stirred at 0 °C for 30 min. 2,6-Dibromopyridine **5** (5.15 g, 21.8 mmol) and $Pd(PPh_3)_4$ (0.250 g, 0.01 mmol%) were then directly added, and the mixture was heated to reflux for 48 h. The course of the reaction was followed by TLC (*n*-hexane/AcOEt, 4:1). Water was added at room temperature, and the product was extracted with AcOEt. The solvents were evaporated and the major product was purified by flash chromatography (*n*-hexane/AcOEt, 5:1) to afford a yellow solid that was recrystallized in pentane/CH_2Cl_2 to afford 4.40 g (66%) of pure **7**. White solid, m.p. 91–92 °C; ^{1}H NMR (200 MHz, $CDCl_3$): $\delta = 8.00$ (dt, $J = 8.4$, 1.8, 1.8 Hz, 2H), 7.67 (dd, $J = 7.7$, 1.1 Hz, 4H), 7.40 (dd, $J = 7.8$, 1.0 Hz, 1H), 5.87 (s, 1H), 4.10 (m, 4H); MS (EI): *m*/*z*: 306, 304 $[M-H]^+$, 235, 233, 154; calcd for $C_{14}H_{12}BrNO_2$: 306.2. 2,6-Di-(*p*-phenyl-1,3-dioxolane)pyridine (10%) and 4,4′-di-(1,3-dioxolane)biphenyl (5%) were also isolated as byproducts.

6,6′-Di-(*p*-phenyl-1,3-dioxolane)-2,2′-bipyridine (8): A solution of *n*BuLi (1.6 M, 1.44 mL, 2.1 mmol) in hexane was added to a solution of **7** (0.612 g, 2 mmol) in Et_2O (20 mL) under argon at −60 °C, and the resulting mixture was stirred for 30 min. Anhydrous $CuCl_2$ (0.1484 g, 1.1 mmol) was then added at −90 °C. The vigorously stirred suspension was allowed to warm up to −70 °C; at this temperature an exothermic reaction took place. Stirring was continued for 1 h, and dry oxygen was bubbled through the solution until the brown suspension turned green (ca. 20 min). The suspension was then hydrolyzed with water (ca. 10 mL), the ether was removed under reduced pressure, and KCN was dissolved in the stirred aqueous solution to remove all the copper. The precipitated solid was filtered off and purified by silicagel chromatography (CH_2Cl_2/MeOH, 0–2%) to yield 0.325 g (72%) of product as a white solid. M.p. 320 °C (decomp); ^{1}H NMR (200 MHz, $CDCl_3$): $\delta = 8.59$ (d, $J = 7.7$ Hz, 2H), 8.18 (d, $J = 8.2$ Hz, 4H), 7.91 (t, $J = 7.7$ Hz, 2H), 7.78 (d, $J = 7.8$ Hz, 2H), 7.62 (d, $J = 8.2$ Hz, 4H), 5.92 (s, 2H), 4.10 (m, 8H); ^{13}C NMR ($CDCl_3$): $\delta = 190.8$ (s, 2C), 156.0 (s, 2C), 140.3 (s, 2C), 138.7 (s, 2C), 137.6 (d, 2C), 127.0 (d, 4C), 126.8 (d, 4C), 120.4 (d, 2C), 119.7 (d, 2C), 103.5 (d, 2C), 65.3 (t, 4C). FAB$^+$-MS: *m*/*z*: 453 $[M+H]^+$, 365, 307; calcd for $C_{28}H_{24}N_2O_4$: 452.6.

6,6′-di-(*p*-formylphenyl)-2,2′-bipyridine (2): A solution of 5% HCl in water (ca. 5 mL) was added to **8** (0.300 g, 0.66 mmol), and the suspension was stirred at room temperature for 12 h. A solid was recovered by filtration, washed with cold water, and dried to yield the monohydrochloride salt of **2**. ^{1}H NMR (200 MHz, [D$_6$]DMSO): $\delta = 10.10$ (s, 2H), 8.64 (d, $J = 7.1$ Hz, 2H), 8.50 (d, $J = 7.8$ Hz, 4H), 8.21 (t, $J = 7.6$ Hz, 4H), 8.08 (d, $J = 7.8$ Hz, 4H), 7.21 (s, $J = 5.3$ Hz, N_2H^+). A suspension of this salt in water was neutralized with aq. $NaHCO_3$, and extracted with CH_2Cl_2. The organic layer was dried and concentrated in vacuo to afford **2**, which was purified by silicagel chromatography (CH_2Cl_2/MeOH, 0–10%). Yield, 0.227 g (94%); white solid, m.p. 260 °C (decomp); ^{1}H NMR ($CDCl_3$, 200 MHz): $\delta = 10.12$ (s, 2H), 8.68 (dd, $J = 7.6$, 0.8 Hz, $H_{3,3'}$), 8.36 (d, $J = 8.3$ Hz, 4H), 8.04 (d, $J = 8.3$ Hz, 4H), 8.00 (t, $J = 7.7$ Hz, $H_{4,4'}$), 7.89 (dd, $J = 7.7$, 0.8 Hz, $H_{5,5'}$); ^{13}C NMR ($CDCl_3$): $\delta = 192.0$ (d, 2C), 155.9 (s, 2C), 154.9 (s, 2C), 144.8 (s, 2C), 138.0 (d, 2C), 136.5 (s, 2C), 130.2 (d, 4C), 127.5 (d, 4C), 121.2 (d, 2C), 120.6 (d, 2C); DCI-MS: *m*/*z*: 365 $[M+H]^+$; calcd for $C_{24}H_{16}N_2O_2$: 364.5.

Bis-porphyrin 2Hphen2H: Three drops of trifluoroacetic acid were added to a solution of **1** (0.088 g, 0.224 mmol), **3** (0.390 g, 1.79 mmol), and **4** (0.514 g, 2.24 mmol) in CH_2Cl_2 (250 mL) under argon. The reaction mixture was stirred at room temperature for 16 h. Subsequently, solid chloranil (1.59 g, 6.88 mmol) was added, and the reaction mixture refluxed for 1.5 h. It was quenched with 10% aqueous $NaHCO_3$. The organic layer was washed with water and evaporated to dryness. The crude product was extracted with hexane and chromatographed on an alumina column and eluted with a mixture of hexane and dichloromethane (130:70), providing the bis-porphyrin 2Hphen2H in pure form. The residue, which contained small amounts of bis-porphyrin was subjected to successive column chromatographies on alumina and silica, using *n*-hexane/CH_2Cl_2 mixtures as eluents. The total yield of 2Hphen2H was 0.055 g (15%). ^{1}H NMR (200 MHz, $CDCl_3$): $\delta = 10.17$ (s, 4H, meso), 9.02 (d, $J = 8.1$ Hz, 4H; H_o), 8.52 (AB, $\Delta\tilde{\nu} = 4.5$ Hz, $J = 7$ Hz, 4H; $H_{3,8}$, $H_{4,7}$), 8.30 (d, $J = 8.1$ Hz, 4H; H_m), 7.96 (s, 2H; $H_{5,6}$), 7.87 (d, $J = 1.7$ Hz, 4H; H_{op}), 7.78 (t, $J = 1.8$ Hz, 2H; H_{pp}), 3.99 (m, 16H; CH_{2b}, CH_{2c}), 2.63 (s, 12H; CH_{3d}), 2.41 (s, 12H; CH_{3a}), 1.72 (t, $J = 7.4$ Hz, 24H; CH_{3b}, CH_{3c}), 1.47 (s, 36H; *t*Bu), −2.46 (s, 4H; NH). FAB$^+$-MS: *m*/*z*: 1663.0, 831.5; calcd for $C_{116}H_{128}N_{10}$: 1664.4 $[M+H]^+$, 832.0 ($[M+2H]^+/2$); UV/Vis (CH_2Cl_2): $\lambda = 273$, 409, 507, 540, 573, 625 nm (plus an impurity at 654 nm).

Bis-porphyrin Znphen2H: A solution of $Zn(OAc)_2 \cdot 2H_2O$ (0.0072 g, 0.033 mmol) in CH_3OH (7 mL) was added to a refluxing solution of 2Hphen2H (0.055 g, 0.033 mmol) in $CHCl_3$ (20 mL) under argon over 20 min. The reaction mixture was refluxed for 1.5 h. The solvents were rotary evaporated, and the residue redissolved in CH_2Cl_2 (70 mL) and shaken with a 5% aqueous solution in of $NaHCO_3$ (80 mL). The organic layer was washed with water and evaporated to dryness. Examination of the residue by TLC (Al_2O_3, *n*-hexane/CH_2Cl_2, 50:50) showed three spots, corresponding to the bis-porphyrins 2Hphen2H, Znphen2H, and ZnphenZn in the order of increasing polarity. The products were separated by successive column chromatographies on alumina and silica, with *n*-hexane/CH_2Cl_2 mixtures as eluents. The yields obtained were 0.0137 g (18%) for 2Hphen2H, 0.0147 g (25%) for ZnphenZn, and 0.0231 g (41%) for Znphen2H.

ZnphenZn: ^{1}H NMR (200 MHz, $CDCl_3$): $\delta = 10.13$ (s, 4H, meso), 9.06 (d, $J = 8.2$ Hz, 4H; H_o), 8.56 (AB, $\Delta\tilde{\nu} = 15$ Hz, $J = 8.6$ Hz, 4H; $H_{3,8}$, $H_{4,7}$), 8.32 (d, $J = 8.2$ Hz, 4H; H_m), 7.97 (s, 2H; $H_{5,6}$), 7.87 (d, $J = 1.8$ Hz, 4H; H_{op}), 7.77 (t, $J = 1.8$ Hz, 2H; H_{pp}), 3.96 (m, 16H; CH_{2b}, CH_{2c}), 2.61 (s, 12H; CH_{3d}), 2.38 (s, 12H, CH_{3a}), 1.71 (t, $J = 7.5$ Hz, 24H; CH_{3b}, CH_{3c}), 1.47 (s, 36H, *t*Bu); FAB$^+$-MS: *m*/*z*: 1787.7, 894.3; calcd for $C_{116}H_{124}N_{10}Zn_2$: 1789.0 $[M+H]^+$, 894.5 ($[M+2H]^+/2$); UV/Vis (CH_2Cl_2): $\lambda = 273$, 342, 413, 542, 575 nm.

Znphen2H: ^{1}H NMR (200 MHz, $CDCl_3$): $\delta = 10.17$ (s, 2H; meso′), 10.14 (s, 2H; meso), 9.05 (d, $J = 8.3$ Hz, 2H; H_o), 9.02 (d, $J = 8.3$ Hz, 2H; $H_{o'}$), 8.55 (AB, 2H, $H_{3,8}$), 8.52 (AB, 2H, $H_{4,7}$), 8.33 (d, $J = 6.5$ Hz, 2H; H_m), 8.30 (d, $J = 8.1$ Hz, 2H; $H_{m'}$), 7.95 (s, 2H; $H_{5,6}$), 7.88 (d, $J = 1.8$ Hz, 2H; H_{op}), 7.86 (d, $J = 1.8$ Hz, 2H; $H_{op'}$), 7.78 (t, 2H; H_{pp}, $H_{pp'}$), 3.97 (m, 16H; CH_{2b}, CH_{2c}, $CH_{2b'}$, $CH_{2c'}$), 2.62 (s, 12H; CH_{3d}, $CH_{3d'}$), 2.41 (s, 6H, $CH_{3a'}$), 2.39 (s, 6H, CH_{3a}), 1.72 (t, $J = 7.3$ Hz, 12H; CH_{3b}, CH_{3c}, $CH_{3b'}$, and $CH_{3c'}$), 1.47 (s, 18H; *t*Bu, *t*Bu′), −2.65 (s, 2H; NH); FAB$^+$-MS: *m*/*z*: 1725.9, 862.9; calcd for

0947-6539/99/0507-2098 $ 17.50+.50/0 *Chem. Eur. J.* **1999**, *5*, No. 7

$C_{116}H_{126}N_{10}Zn$: 1725.7 $[M+H]^+$, 863.0 ($[M+2H]^+/2$); UV/Vis (CH_2Cl_2): $\lambda = 273$, 412, 507, 541, 574, 624 (impurity at 653 nm).

Bis-porphyrin 2Hbipy2H: A mixture of **2** (0.071 g, 0.19 mmol), **4** (0.450 g, 1.95 mmol), and **3** (0.342 g, 1.56 mmol) in dichloromethane (180 mL) was degassed with argon. After addition of five drops of trifluroacetic acid, the resulting solution was stirred at room temperature for 17 h. Oxidation was performed with the use of chloranil (2.30 g, 9.4 mmol) and by heating the reaction mixture under reflux for two hours. The solution was then neutralized with aq. 10% Na_2CO_3. The resulting organic phase was washed three times with water and evaporated to dryness. The residue was submitted to several chromatographies (SiO_2, CH_2Cl_2, then fine SiO_2, $CHCl_3$), to afford 0.063 g (20% yield) of the desired compound. ^{1}H NMR ($CDCl_3 + 2$ drops of CF_3CO_2D): $\delta = 10.55$ (4H; meso), 8.94–8.83 (m, 10H; H_o, H_m, $H_{3,8}$, $H_{4,7}$, $H_{5,6}$), 8.27 (s, 2H; H_{pp}), 8.20 (s, 4H; H_{op}), 3.86 (s, 16H; CH_{2a}, CH_{2b}), 2.49 (s, 12H; CH_{3a}), 2.40 (s, 12H; CH_{3d}), 1.65 (s, 36H; *t*Bu), 1.45 (m, 24H; CH_{3b}, CH_{3c}); FAB$^+$-MS: *m*/*z*: 1639.0, 820.0; calcd for $C_{114}H_{128}N_{10}$: 1639.4 $[M+H]^+$, 820.2 ($[M+2H]^+/2$); UV/Vis ($CHCl_3$): $\lambda =$ 412, 508, 541, 574, 625 nm.

Bis-porphyrin Znbipy2H: A degassed solution of $Zn(OAc)_2 \cdot 2H_2O$ (0.0093 g, 0.042 mmol) in methanol (13 mL) was added under argon to a solution of 2Hbipy2H (0.063 g, 0.038 mmol) in chloroform (45 mL). This mixture was heated under reflux for two hours. After evaporation of the solvents, the residue was purified by column chromatography. A first separation on silica (hexane/$CHCl_3$, 3:1) afforded ZnbipyZn (32%) and a mixture of 2HbipyZn and 2Hbipy2H. This mixture could be separated on a second silicagel column. Znbipy2H was eluted with CH_2Cl_2/acetone (97:3) and obtained in 24% yield (0.012 g). Analytical data (NMR spectra could not be obtained, due to the insolubility of the samples in non protic solvents):

ZnbipyZn: FAB$^+$-MS: *m*/*z*: 1764.7; calcd for $C_{114}H_{124}N_{10}Zn_2$: 1765 $[M+H]^+$; UV/Vis ($CHCl_3$): $\lambda = 413$, 539, 574 nm.

Znbipy2H: FAB$^+$-MS: *m*/*z*: 1701.9, 850.4; calcd for $C_{114}H_{126}N_{10}Zn$: 1702 $[M+2H]^+ + e^-$, 851 ($[M+2H]^+/2$); UV/Vis (acetone/$CHCl_3$, 1:1): $\lambda = 413$, 508, 539, 574, 625 nm.

Absorption and fluorescence spectra: The steady state absorption and fluorescence spectra for 5×10^{-5} M solutions of the compounds in dichloromethane were recorded with a Perkin–Elmer Lambda 6 and a Spex Fluorolog spectrometer, respectively. As degassing did not increase the fluorescence quantum yield, the samples were investigated in aerated solution. The fluorescence quantum yield of the model compounds was determined with a solution of cresyl violet in methanol as reference. The excitation wavelength was chosen as at this wavelength a majority (ca. 76%) of the incident light would be absorbed by the zinc porphyrin moiety.

Fluorescence decays: The time-resolved fluorescence measurements were performed with an argon-ion-pumped mode-locked pyrromethane dye laser system with a repetition rate of 820 KHz. The fluorescence signal was detected through a polarizer at the magic angle and a subtractive double monochromator (American Holographic) with a Hamamatsu R2809U microchannel plate photomultiplier.[52, 53] The instrumental response, recorded sequentially after the decay with a scattering solution, was found to have a full width at half maximum of about 80 ps. The determination of the instrumental response function with a scattering solution and with detection of fluorescence by a microchannel plate was justified by the small wavelength range investigated (580 to 695 nm). The fluorescence decays were measured to a precision of 10000 counts in the peak channel and were analyzed as a single exponential decay (model compounds) or as a sum of three our four exponentials (Znphen2H and Znbipy2H) with a nonlinear least-square program with iterative reconvolution [Eq. (15)].[54–56]

$$I(t) = \sum_{i=1}^{n} A_i \exp^{-\lambda_i t} \qquad (15)$$

The goodness of fit was judged in terms of the statistical parameter χ^2 (generally less than 1.2 for an acceptable fit), $Z\chi^2$, the runs-test[57] and the Durbin-Watson parameters,[58] and by visual inspection the weighted residuals and their autocorrelation function.[56] The positive preexponential factors (indicative of the amount of a fluorescence component) were presented normalized to 1 and errors were taken as three standard deviations. To increase the reliability of the analysis the decays were analyzed globally,[59–61] linking the decay times, over two different time increments and/or at three or four different wavelengths as a sum of exponentials. When justified by the proposed kinetic scheme two decay times of the compounds Znbipy2H and Znphen2H were linked to those of the model compounds.

Structure calculations: The geometry of Znphen2H and Znbipy2H was calculated with the Merck Molecular Force Field employed in the Spartan® software package.[62]

Acknowledgments

M.V.d.A. is an Onderzoeksdirekteur of the F.W.O.-Vlaanderen. G. Hungerford acknowledges the Research Council of the K.U.Leuven for a fellowship. The authors gratefully acknowledge the F.W.O., the Nationale Loterij, the continuing support from DWTC (Belgium) through IUAP IV-11, and the European Community through Project: CHRX-CT94-0538 (Human Capital and Mobility).

[1] G. McDermott, S. M. Prince, A. A. Freer, A. M. Hawthornthwaite-Lawless, M. Z. Papiz, R. J. Cogdell, N. W. Isaacs, *Nature* **1995**, *374*, 517–521.
[2] W.Kühlbrandt, *Nature* **1995**, *374*, 497–498.
[3] R. G. Little, *J. Heterocycl. Chem* **1978**, *15*, 203–208.
[4] J. A. Anton, P. A.Loach, R. Govingjee, *Photochem. Photobiol.* **1978**, *28*, 235–242.
[5] J.Mårtensson, K. Sandross, O. Wennerström, *Tetrahedron Lett.* **1993**, *34*, 541–544.
[6] A. Osuka, K. Maruyama, I. Yamazaki, N. Tamai, *J. Chem. Soc. Chem. Commun.* **1988**, 1243–1245.
[7] A. Osuka, K. Maruyama, I. Yamazaki, N. Tamai, *Chem. Phys. Lett.* **1990**, *165*, 392–396.
[8] N. Nagata, A. Osuka, K. Maruyama, *J. Am. Chem. Soc.* **1990**, *112*, 3054–3059.
[9] S. Chardon-Noblat, J.-P.Sauvage, *Tetrahedron* **1991**, *47*, 5123–5132.
[10] E. J. Atkinson, A. M. Oliver, M. N. Paddon-Row, *Tetrahedron Lett.* **1993**, *34*, 6147–6150.
[11] R. W. Wagner, T. E. Johnson, J. S. Lindsey, *J. Am. Chem. Soc.* **1996**, *118*, 11166–11180.
[12] H. L. Anderson, C. A. Hunter, J. K. M. Sanders, *J. Chem. Soc. Chem. Commun.* **1989**, 226–227.
[13] J.-P. Collin, V. Heitz, J.-P. Sauvage, *Tetrahedron Lett.* **1991**, *32*, 5977–5980.
[14] U. Rempel, B. von Maltzan, C. von Bosczyskowski, *Pure Appl. Chem.* **1993**, *65*, 1681–1685.
[15] A. V. Chernook, A. M. Shulga, E. I. Zenkevich, U. Rempel, C. von Borczyskowski, *Ber. Bunsenges. Phys. Chem.* **1996**, *100*, 2065–2069.
[16] H. Hunter, R. Hyde, *Angew. Chem.* **1996**, *108*, 2064–2067; *Angew. Chem. Int. Ed. Engl.* **1996**, *35*, 1936–1939.
[17] A. Harriman, D. J. Magda, J. L. Sessler, *J. Chem. Soc. Chem. Commun.* **1991**, 345–348.
[18] J. L. Sessler, B. Wang, A. Harriman, *J. Am. Chem. Soc* **1995**, *117*, 704–714.
[19] S. Prathapan, T. E. Johnson, J. S. Lindsey, *J. Am. Chem. Soc.* **1993**, *115*, 7519–7520.
[20] D. W. J. McCallien, J. K. M. Sanders, *J. Am. Chem. Soc.* **1995**, *117*, 6611–6112.
[21] A. V. Chernook, A. M. Shulga, E. I. Zenkevich, U. Rempel, C. von Borczyskowski, *J. Phys. Chem.* **1996**, *100*, 1918–1926.
[22] R. V. Slone, J. T. Hupp, *Inorg. Chem.* **1997**, *36*, 5422–5423.
[23] S. Anderson, H. L. Anderson, A. Bashall, M. McPartlin, J. K. M. Sanders, *Angew. Chem.* **1995**, *107*, 1196–1200; *Angew. Chem. Int. Ed. Engl.* **1995**, *34*, 1096–1099.
[24] J.-C. Chambron, V. Heitz, J.-P. Sauvage, J.-L. Pierre, D. Zurita, *Tetrahedron Lett.* **1997**, *36*, 9321–9324.
[25] J. E. Parks, B. E. Wagner, R. H. Holm, *J. Organomet. Chem.* **1973**, *56*, 53–66.
[26] E. Bullock, A. W. Johnson, E. Markham, K. B. Shaw, *J. Chem. Soc.* **1958**, 1430–1440.
[27] R. Young, C. K. Chang, *J. Am. Chem. Soc.* **1985**, *107*, 898–909.

[28] J. S. Lindsey, H. C. Hsu, I. C. Schreiman, *Tetrahedron Lett.* **1986**, *27*, 4969 – 4970.
[29] J. S. Lindsey, I. C. Schreiman, H. C. Hsu, P. C. Kearney, A. M. Marguerettaz, *J. Org. Chem.* **1987**, *52*, 827 – 836.
[30] G. P. Arsenault, E. Bulloch, S. F. McDonald, *J. Am. Chem. Soc.* **1960**, *82*, 4384 – 4389.
[31] A. Agresti, M. Bacci, E. Castellucci, P. R. Salvi, *Chem. Phys. Lett.* **1982**, *89*, 324 – 328.
[32] V. Barone, C. Minichino, S. Fliszàr, N. Russo, *Can. J. Chem.* **1988**, *66*, 1313 – 1317.
[33] A. Almenningen, O. Bastiansen, S. Gundersen, S. Samdal, *Acta Chem. Scand.* **1989**, *43*, 932 – 937.
[34] J. E. Löfroth, *Anal. Instrum.* ***1985****, 14, 403 – 431.*
[35] M. Ameloot, N. Boens, R. Andriessen, V. Van den Bergh, F. C. De Schryver, *J. Phys. Chem.* **1991**, *95*, 2041 – 2047.
[36] R. Andriessen, N. Boens, M. Ameloot, F. C. De Schryver, *J. Phys. Chem.* **1991**, *95*, 2047 – 2058.
[37] Z. Pawelka, L. Sobczk, *Bull. Acad. Pol. Sci.* **1976**, *24*, 961.
[38] R. Benedix, P. Birner, F. Birnstock, H. Hennig, H.-J. Hofmann, *J. Mol. Struct.* **1979**, *51*, 99 – 105.
[39] J. Mårtensson, *J. Chem. Phys. Lett.* **1994**, *229*, 449 – 456.
[40] V. Czikkelly, H. D. Försterling, H. Kuhn, *Chem. Phys. Lett.* **1970**, *6*, 207 – 210.
[41] V. Czikkelly, H. D. Försterling, H. Kuhn, *Chem. Phys. Lett*. **1970**, *6*, 11 – 14.
[42] B. Norland, A. Ames, T. Taylor, *Photogr. Sci. Eng.* **1970**, *14*, 295 – 307.
[43] J. C. Chang, *J. Chem. Phys.* **1977**, *67*, 3901 – 3909.
[44] G. D. Scholes, K. P. Ghiggino, *J. Phys. Chem.* **1994**, *98*, 4580 – 4590.
[45] G. D. Scholes, *J. Phys. Chem.* **1996**, *100*, 18731 – 18739.
[46] R. D. Harcourt, G. D. Scholes, K. P. Ghiggino, *J. Chem. Phys.* **1994**, *101*, 10521 – 10525.
[47] D. L. Dexter, *J. Chem. Phys.* **1953**, *21*, 836 – 850.
[48] A. H. A. Clayton, G. D. Scholes, K. P. Ghiggino, M. N. Paddon-Row, *J. Phys. Chem.* **1996**, *100*, 10912 – 10918.
[49] J. S. Lindsey *J. Am. Chem. Soc.* **1996**, *118*, 11181 – 11193.
[50] P. Karafiloglou, *Chem. Phys.* **1997**, *214*, 171 – 182.
[51] P. Karafiloglou, J. *Molecular Structure (Theochem)* **1998**, *428*, 221 – 229.
[52] D. V. O'Connor, D. Phillips, *Time-correlated Single Photon Counting*, Academic Press, London, **1984**.
[53] M. M. Khalil, N. Boens, M. Van der Auweraer, M. Ameloot, R. Andriessen, J. Hofkens, F. C. De Schryver, *J. Phys. Chem.* **1991**, *95*, 9375 – 9381.
[54] R. F. Gunst, R. L. Mason, *Regression Analysis and its Application, A Data-Oriented Approach*, Marcel Dekker, New York **1980**.
[55] D. W. Marquardt, *J. Soc. Ind. Appl. Math.* **1963**, *11*, 431 – 441.
[56] A. Grinvald, I. Z. Steinberg, *Anal. Biochem.* **1974**, *59*, 583 – 598.
[57] D. Caterall, in *Time-resolved Spectroscopy in Biochemistry and Biology* (Eds.: R. B. Cundall, R.E Dale), Plenum, New York **1983**.
[58] J. Durbin, G. S. Watson, *Biometrika* **1950**, *37*, 409 – 416; J. Durbin, G. S. Watson, *Biometrika* **1951**, *38*, 159 – 178; J. Durbin, G. S. Watson, *Biometrika* **1971**, *58*, 1 – 19.
[59] J. M. Beechem, M. Ameloot, L. Brand, *Chem. Phys. Lett.* **1985**, *120*, 466 – 472.
[60] N. Boens, L. D. Janssens, F. C. De Schryver, *Biophys. Chem.* **1989**, *33*, 77 – 90.
[61] L. D. Janssens, N. Boens, M. Ameloot, F. C. De Schryver, *J. Phys. Chem.* **1990**, *94*, 3564 – 3576.
[62] W. J. Hehre, Spartan, version 4.0, © **1995**, Wavefunction, Inc.

Received: November 3, 1998 [F1423]

  0947-6539/99/0507-2100 $ 17.50+.50/0